Hindawi Publishing Corporation
International Journal of Photoenergy
Volume 2013, Article ID 245646, 8 pages
http://dx.doi.org/10.1155/2013/245646

Research Article

Multifunctional Chitosan-Copper Oxide Hybrid Material: Photocatalytic and Antibacterial Activities

Yuvaraj Haldorai and Jae-Jin Shim

School of Chemical Engineering, Yeungnam University, Gyeongsan, Gyeongbuk 712-749, Republic of Korea

Correspondence should be addressed to Yuvaraj Haldorai; yuvraj_pd@yahoo.co.in

Received 28 May 2013; Accepted 18 August 2013

Academic Editor: Meenakshisundaram Swaminathan

Chitosan (CS) anchored copper oxide (CuO) hybrid material was prepared by chemical precipitation method. Fourier transform infrared spectroscopy (FT-IR) and X-ray diffraction (XRD) confirmed the formation of CS-CuO hybrid. Transmission electron microscopy (TEM) analysis showed the immobilization of CuO nanoparticles on the surface of CS. The hybrid was also characterized by thermogravimetric analysis (TGA) and zeta potential. The hybrid exhibited high photocatalytic activity as evident from the degradation of methylene blue (MB) dye. The result revealed substantial degradation of the MB dye (84%) under UV-light illumination. The antibacterial activity of hybrid against *Escherichia coli* was examined by colony forming units. It was proved that the CS encapsulated CuO hybrid exhibited excellent antibacterial activity.

1. Introduction

In general, nanotechnology can be understood as a technology of design, fabrication, and applications of nanostructures and nanomaterials. Nanometer size structures are an intermediate form of matter which exhibit exotic physical and chemical properties different from those observed in bulk three-dimensional materials. Nanoscale oxides of transition metals are gaining continuous importance for various applications such as catalysts, passive electronic components, and ceramic materials [1, 2]. From an environmental standpoint, heterogeneous photocatalysis is a significant cutting-edge technology for application in water purification [3]. The interest in the study of biopolymer has witnessed a steady increase, because they are environmentally friendly alternatives to synthetic, nonbiodegradable polymers. However, the poor regeneration and reuse of biopolymers have limited their adsorption properties, which may be improved by adding reinforcing compounds (fillers) and forming composites [4]. The immobilization of an appropriate catalyst onto the surface of a natural biopolymer provides a number of additional advantages including low-cost, high adsorption, high catalytic activity, and extensive potential for reuse [5].

In this regard, chitosan (CS), a linear cationic, pH sensitive, nontoxic, biodegradable, biocompatible polysaccharide obtained from deacetylation of chitin seems to offer numerous distinct advantages [6]. CS is a super high-capacity adsorbent for contaminant removal in water with adsorption capacity of 1000–1100 g Kg^{-15} which is higher than the activated carbon [7]. This high adsorption of CS is due to the binding ability of CS with contaminants through hydroxyl and amino groups on the surface. The regeneration of CS by acid or base is a simple and cost effective, but the application of acid or base for CS regeneration is not technically advantageous. The large amount of wastewater generated from regeneration process needs further treatment making the process unsustainable [8, 9]. So, the immobilization of photocatalyst onto the CS aids in removal of contaminants adsorbed by the CS and also gives antibacterial materials with improved functional properties.

Cupric oxide (CuO), a p-type semiconductor with monoclinic structure is an interesting multifunctional material due to its promising applications in magnetic storage, solar energy transformation, electronics, sensors, batteries, and catalysis [10]. CuO crystal structure possesses a narrow band gap due to which it has useful photocatalytic or photovoltaic properties as well as photoconductive functionalities [11]. CuO nanoparticles with various morphologies have been developed by numerous methods like oxidation of copper at

high temperature, reverse micelle, surfactant templates, solid state reactions, hydrothermal and thermal decomposition method [10, 12–15]. The immobilization of CuO onto CS resolves the recollection and reuses limitation of CuO to remove the contaminants adsorbed by CS *in situ* without use of acid or base and generating secondary pollutants and sterilizes pathogens. Recently, Gouda and Hebeish [16] prepared chitosan/CuO nanocomposite and investigated its antibacterial activity.

In this study, we synthesized a multifunctional material CS-CuO to meet the need of high adsorption, self-regeneration, easy separation, and cost-effective dye removal from aqueous solution with enhanced antimicrobial property. The CS-CuO hybrid synthesized by precipitation method is characterized by FT-IR, XRD, zeta potential, and TEM. The CS-CuO hybrid as a reusable photocatalyst was examined through photodegradation of MB dye. The high antibacterial activity of CS-CuO hybrid against *E. coli* is explored. Thus this novel CS-CuO hybrid has great potential to be used as an economic, environmental friendly, and sustainable material for dye removal with enhanced antimicrobial activity.

2. Experimental

2.1. Materials. Chitosan (CS) with degree of acetylation 85% and molecular weight 2.6×10^5 was purchased from Aldrich. Copper nitrate trihydrate ($Cu(NO_3)_2{\cdot}3H_2O$), sodium hydroxide (NaOH), acetic acid (CH_3COOH), and methylene blue (MB) were of analytical grade and purchased from Aldrich. Beef extract, peptone, and agar powder were of bacteriological grade, and *Escherichia coli* (*E. coli*) (KCCM 12119) was used as a model organism for evaluation of the antibacterial activity. Deionized water was used throughout the studies.

2.2. Preparation of CS-CuO Hybrid. The CS-CuO hybrid was prepared according to the procedure given in the literature [17]. In a typical experiment, 1 g of CuO nanoparticles prepared by thermal decomposition of $Cu(NO_3)_2{\cdot}3H_2O$ at 350°C for 2 h was dispersed in 100 mL of 1% (v/v) acetic acid, where CuO changed into copper cations. To this, 1 g of CS was added and sonicated for 30 min and stirred continuously until the clear sol was obtained. NaOH solution (1 M) was then added dropwise until the solution attained pH 10. The precipitate obtained was heated at 80°C for 5 h and then filtered, washed with excess of water and dried in a vacuum oven at 60°C for overnight.

2.3. Photocatalytic Degradation of MB Dye. Methylene blue (MB) dye was used as a probe molecule to evaluate the photocatalytic activity of hybrid. The photocatalytic reaction was conducted at room temperature under UV light at a wavelength of 365 nm. In a typical experiment, 0.4 mg of CS-CuO hybrid was added into the water (10 mL) containing 0.2 mg of MB dye, followed by the addition of 1 mL H_2O_2. Prior to the irradiation, the suspension was magnetically stirred in the dark for 30 min to establish the adsorption/desorption equilibrium of MB. A 2 mL of the sample was withdrawn for every 10 min. Before analysis, the suspension was centrifuged to remove any suspended solid catalyst. The residual concentration of dye was measured using a Jasco V-650 UV-visible spectrophotometer.

2.4. Antibacterial Activity. *E. coli* was grown in a nutrient agar (DIFCO 0001) containing 3 g/L beef extract, 5 g/L peptones, and 15 g/L agar in distilled water. pH of the medium was adjusted to 7.0. The antibacterial activity of the CS-CuO hybrid was evaluated through colony forming units (CFU) count method. Freeze-dried sample of hybrid was sliced into small pieces and sterilized at 121°C for 15 min. 9 mL of the growth medium for *E. coil* was added to separate test tubes, and 0.03 g/mL of finely sliced solid hybrid samples was added to each of the test tubes. The tubes were then seeded with 1 mL fresh culture of *E. coli* and incubated at 37°C for 12 h. Samples were taken after 6, 12, 18, and 24 h for CFU determination. The sample was diluted with saline water and cultured on agar plates for 12 h. The CFU was determined by counting the colonies on agar plates, and mean values were presented from at least 3 experiments.

2.5. Characterization. Fourier transform infrared (FT-IR) spectroscopy was performed using a Jasco FT/IR-620 FT-IR spectrometer. The phase and crystallinity were characterized by using a Rigaku D/max-2500 X-ray diffractometer (XRD) with Cu Kα radiation in the 2θ range of 10–80°. Thermogravimetric analysis (TGA) was performed on a Setaram thermal analyzer (TGA-DSC EVO, France) from 20 to 800°C at a heating rate of 10°C/min under nitrogen atmosphere. Zeta potential analysis was measured using a Malvern Zetasizer Nano instrument with a laser light of wavelength 633 nm at 25°C under the Smoluchowski approximation. Microscopic images were obtained using a Hitachi H-7600 transmission electron microscope with an accelerating voltage of 100 kV. Ultraviolet-visible spectra (UV-vis) were recorded using a Jasco V-650 spectrophotometer.

3. Results and Discussion

Scheme 1 shows the proposed mechanism for the formation of CS-CuO hybrid. The process involved two steps. The first step is the dispersion of CS and CuO nanoparticles in acetic acid solution, where CuO dissolved and changed into copper cations (Cu^{2+}). The Cu^{2+} ions immediately formed coordination bonds with –OH and $-NH_2$ groups of CS chains [18]. In the second step, pH of the solution was increased to 10 by the dropwise addition of NaOH. The precipitate obtained was heated at 80°C for 5 h, where the Cu^{2+} ions transformed into CuO. The possible formation reactions of CuO are given below [19, 20]. The homogeneous dispersion of Cu^{2+} in the CS sol aids in the generation of homogeneous CS-CuO hybrid. Consider

$$\begin{aligned} Cu^{2+} + OH^- &\longrightarrow Cu{-}O{-}H^+ \\ Cu{-}O{-}H^+ + OH^- &\longrightarrow CuO + H_2O \end{aligned} \quad (1)$$

Figure 1 shows the FT-IR spectra of pure CS and CS-CuO hybrid. The spectrum of pure CS exhibited a band

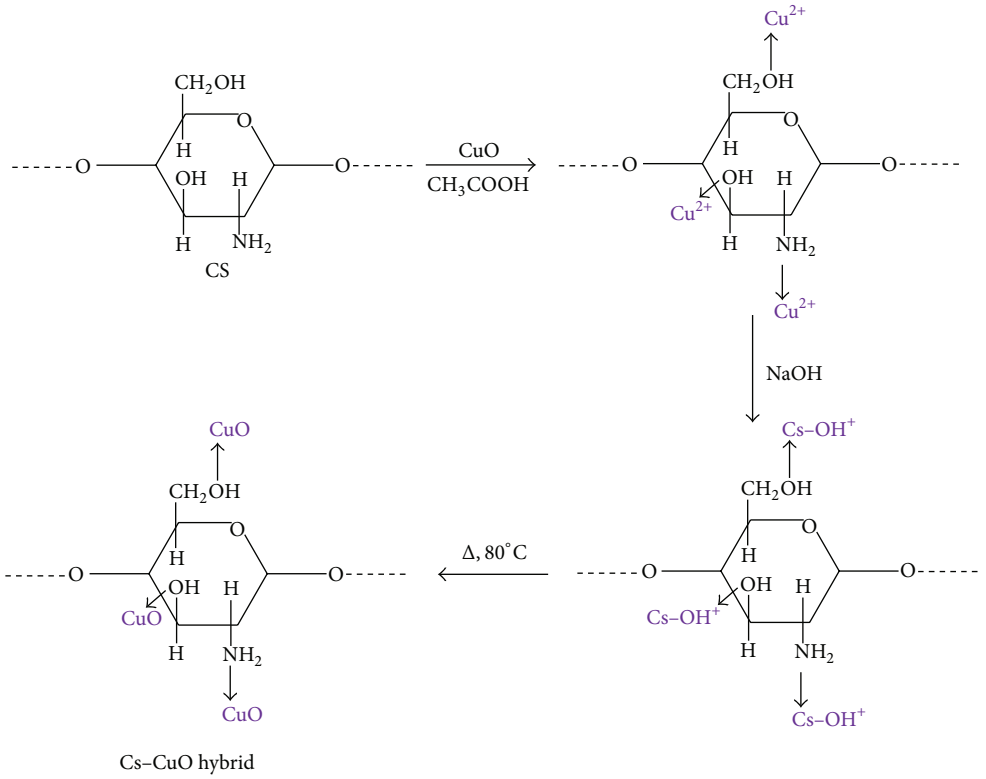

Scheme 1: Schematic representation for the synthesis of CS-CuO hybrid.

at 3370 cm^{-1} was due to the stretching vibrations of –OH and –NH groups. The peak at 2876 cm^{-1} was attributed to the asymmetric stretching of –CH group in polymer, 1650 cm^{-1} indicated the amide I group (C–O stretching along the N–H deformation), 1578 cm^{-1} was due to –NH deformation, 1424 cm^{-1} showed the C–N axial deformation (amine group), 1375 cm^{-1} was attributed to the COO– group in carboxylic acid salt, 1152 cm^{-1} showed the special peak of β(1-4) glycosidic bond in polysaccharide unit, and 1047 cm^{-1} was assigned to the stretching vibration of C–O–C in glucose circle [21]. The CS-CuO hybrid displayed the characteristic bands of both CS and CuO. The band at 520 cm^{-1} was ascribed to the stretching mode of Cu–O [22]. When compared to the pure CS, the bands corresponding to the hydroxyl, amino and amide groups in the spectrum of hybrid were shifted. The shift of IR bands confirmed the interaction between the CS and CuO nanoparticles.

Figure 2 shows the X-ray diffraction patterns of CS and CS-CuO hybrid. The broad peak at 19.77° in the XRD pattern of CS showed that the polymer is amorphous [23]. In the hybrid, we observed both the CS and CuO diffraction peaks. The peaks that appeared at 32.8, 35.9, 36.25, 39.1°, 49.1, 53.5, 58.4, 62.0, 66.4, 68.3, 72.5, and 75.4° in the hybrid were assigned to (110), $(\overline{1}11)$, (111), $(\overline{2}02)$, (020), (202), $(\overline{1}13)$, $(\overline{3}11)$, (220), (311), and (004) planes of CuO with high crystallinity [24]. The diffraction peaks of CuO are in good agreement with the monoclinic CuO (JCPDS card 05-0661). The result proved the successful formation of CS-CuO hybrid.

The thermal stability of CS and CS-CuO hybrid was examined by TGA from 20–800°C under N_2 atmosphere, as illustrated in Figure 3. The two samples followed a similar decomposition trend. The as-synthesized polymer exhibited a two-step weight loss. The first weight loss (around 10%) step in the TGA curve below 100°C was attributed to the loss of water. The second rapid major mass loss step in the range of 200–500°C was assigned to the complex dehydration of the saccharide rings, depolymerization, and decomposition of the acetylated and deacetylated units of the polymer [25]. However, it was found that the thermal stability of hybrid was higher than the pure CS which was obviously related to the existence of thermally stable CuO. The residual mass left at 800°C was found to be 30.4% and 61.5% for the CS and CS-CuO hybrid, respectively.

Zeta potential, that is, surface charge, can greatly influence the particle stability in suspension through electrostatic repulsion between particles. Zeta potential measurement is used to analyze the nanoparticle interaction with the cell membrane of bacteria, which is negatively charged. Figure 4 shows the zeta potential measurement of CS-CuO hybrid. The hybrid has a positive surface charge of about 51.5 mV, while that of CuO has a negative surface charge of –32.1 mV. For CS, the positive zeta potential results from the presence of protonated amine groups. When negatively charged CuO reacts with the positively charged CS, the net zeta potential decreases. The shift may be attributed to the blockage of active sites on the surface of CuO nanoparticles by the adsorption of polymer chain.

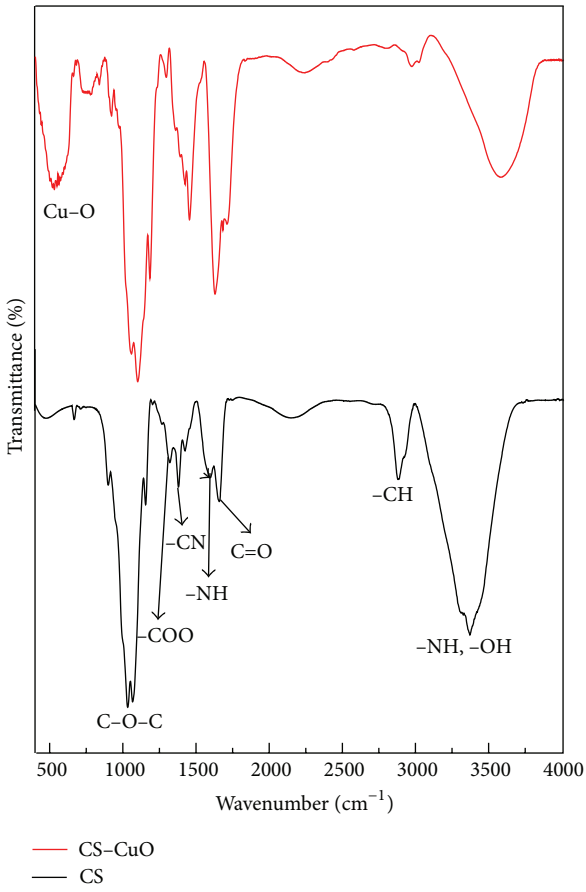

Figure 1: FT-IR spectra of CS and CS-CuO hybrid.

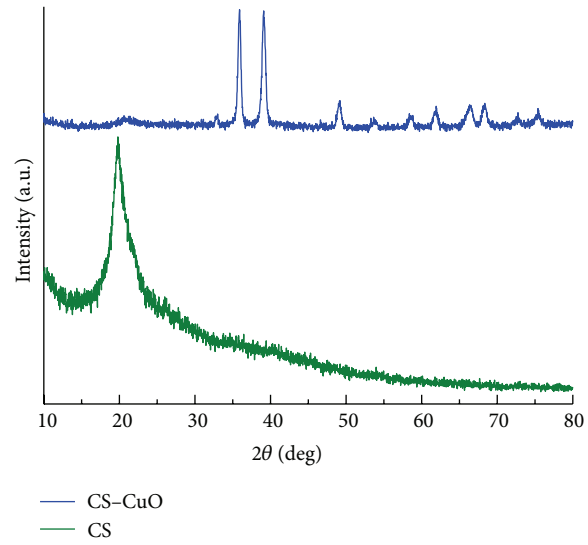

Figure 2: X-ray diffraction patterns of CS and CS-CuO hybrid.

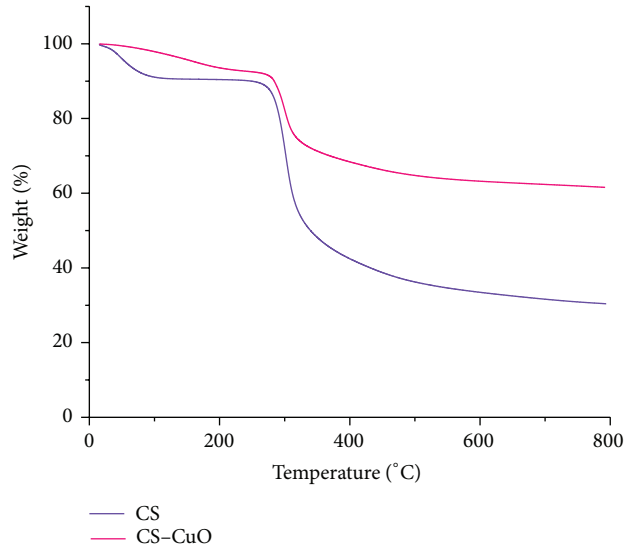

Figure 3: TGA curves of CS and CS-CuO hybrid.

The direct evidence for the immobilization of CuO nanoparticles on the surface of CS was analyzed by TEM (Figure 5). The image showed that the spherical CuO nanoparticles exist on the CS surface with almost uniform distribution. The dark areas represent the crystalline CuO nanoparticles, while the bright areas represent the amorphous CS, owing to the high electron density of the CuO nanoparticles. The interaction between CS and CuO enhanced the properties of CS-CuO hybrid.

As a demonstration of application of such CS-CuO hybrid, MB was chosen as a representative organic dyestuff to evaluate the photocatalytic performance. Figure 6(a) shows the typical time-dependent UV-vis absorption spectra of the MB dye solution during the photodegradation in the presence of CS-CuO hybrid with the aid of H_2O_2. It is seen that dye exhibited a maximum absorption peak at around 653 nm. Note that color of the dye solutions becomes less intense, and the intensity of absorption spectra decreases gradually with increasing the irradiation time, indicating that a strong oxidation of dye has occurred in the presence of CS-CuO hybrid under UV irradiation. All these observations indicated that CS-CuO hybrid exhibited excellent performance for the degradation of dye. Figure 6(b) shows the photocatalytic performance of various catalysts for the degradation of MB dye in the presence of H_2O_2. Approximately 84% of the dye was degraded by the hybrid within 30 min. In the absence of a photocatalyst, the dye was degraded slowly by H_2O_2 (20%). It is seen that the degradation of the dye was greatly enhanced in the presence of photocatalyst, indicating the excellent photocatalytic activity of CS-CuO hybrid. However, the hybrid exhibited no obvious photocatalytic activity in the absence of H_2O_2 (data not shown). According to the previous report [26], the possible mechanism for the degradation of MB dye may be proposed as follows: the photodecomposition of H_2O_2 forms a certain amount of OH radicals in the presence of CuO first, and then these OH radicals degrade the MB dye into CO_2, H_2O, and other mineralization through a series of redox reactions.

On the other hand, there is a possibility of dye degradation by a Fenton-like process. Generally, the Fenton-like process (Cu^{2+}/H_2O_2) showed lower dye degradation than the conventional Fenton reaction (Fe^{2+}/H_2O_2) [27]. In

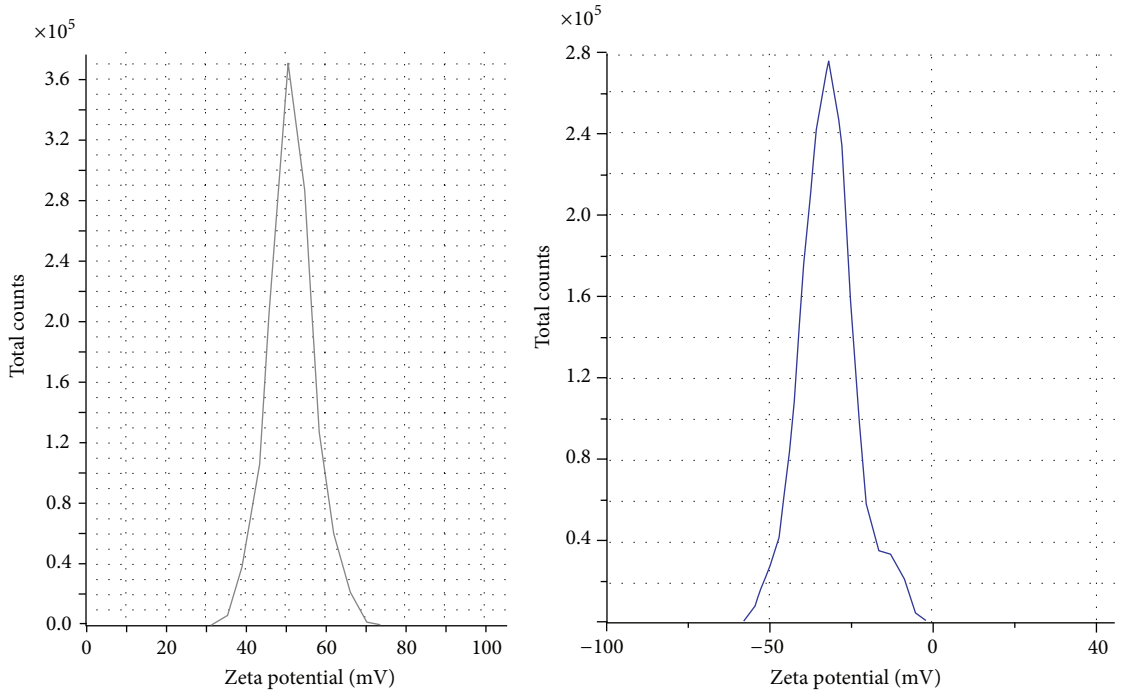

Figure 4: Zeta potential measurement of (a) CS-CuO hybrid and (b) CuO at pH 7.

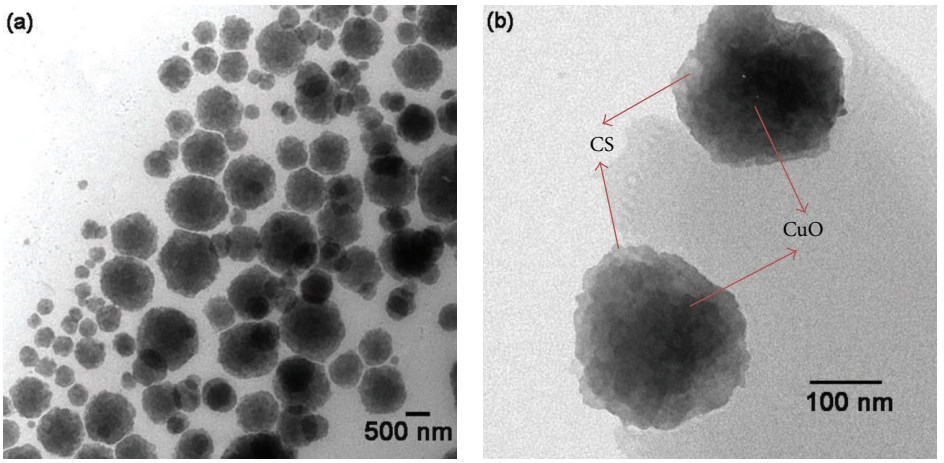

(a) (b)

Figure 5: TEM images of CS-CuO hybrid (a) long view and (b) close inspection.

this system, the Cu^{2+} ions present in the aqueous solution immediately form coordination bonds with –OH and $–NH_2$ groups of CS chains. Therefore, the Cu^{2+} ions were not available for Fenton-like reaction. In other words, there was no direct reaction between Cu^{2+} and H_2O_2.

Furthermore, the photostability of the CS-CuO hybrid was examined based on its photocatalytic performance under UV-light irradiation with three cycles, as shown in Figure 6(c). After three recycles, the catalyst did not exhibit any significant loss of activity, indicating its high stability during photodegradation process.

In general, the kinetics of photocatalytic degradation of organic pollutant on the semiconducting oxide has been established and can be described well by the apparent first order reaction:

$$\ln\left(\frac{C_0}{C}\right) = k_{\text{app}} \times t, \tag{2}$$

where k_{app} is the apparent rate constant, C_0 is the initial concentration of the dye, and C is the concentration of dye at time t.

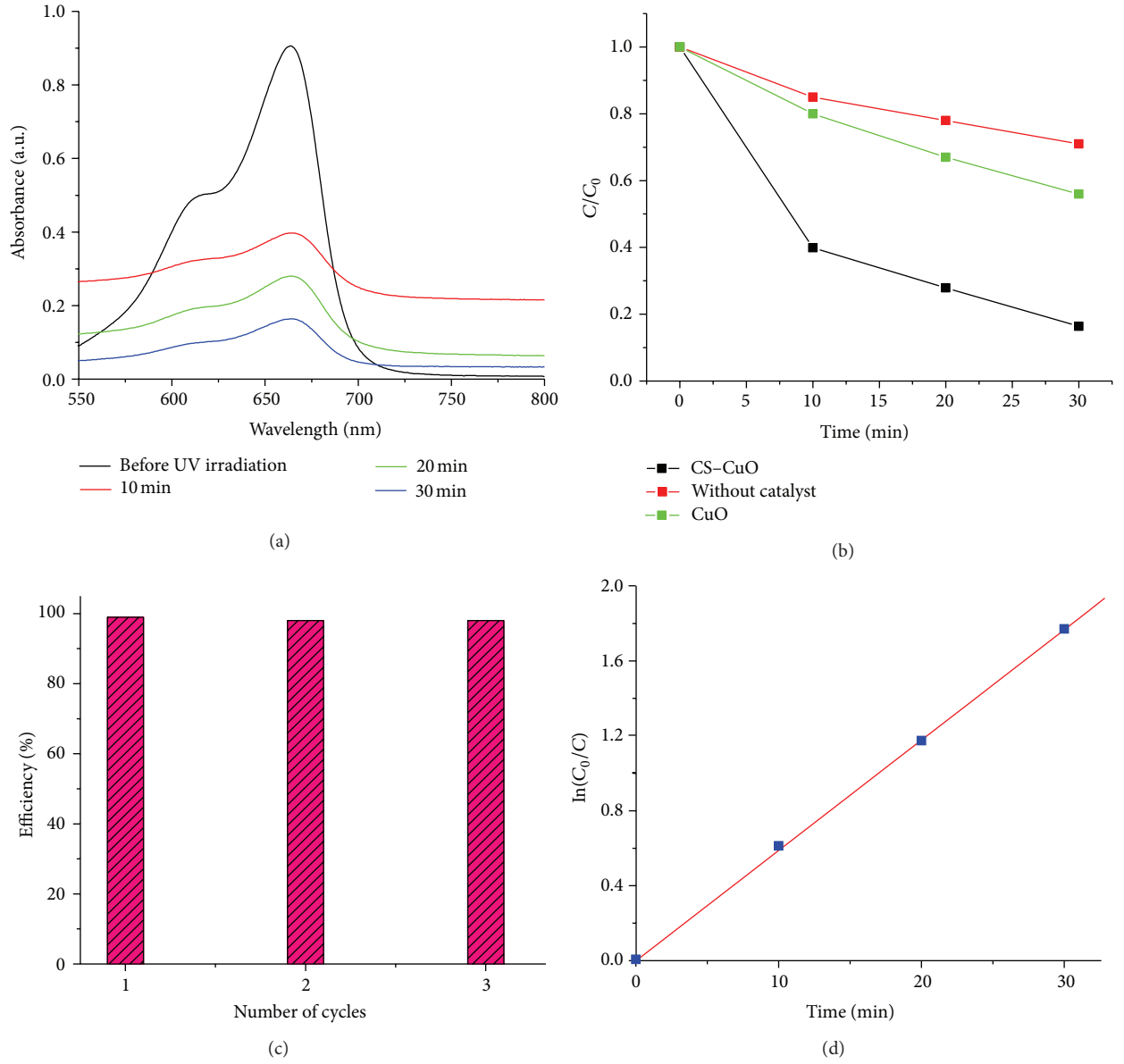

Figure 6: (a) UV-visible spectra of the MB solution in the presence of CS-CuO hybrid at different UV-irradiation time, (b) photodegradation of the MB dye, (c) photostability of the hybrid after three cycles, and (d) first order kinetic model for the photodegradation of MB.

Figure 6(d) shows the apparent rate constant of MB dye in the presence of photocatalyst under UV-light irradiation. The linear correlation of the plot of $\ln(C_0/C)$ versus time suggested a pseudo-first-order reaction for the dye. The apparent rate constant (k_{app}) was determined as 0.059 min^{-1}.

The collective results of the viability of *E. coli* after being treated with CS and CS-CuO hybrid are presented in Table 1. The viable bacteria were monitored by counting the number of CFU. As witnessed from Table 1, it is clear that the control CS sample inactivated the *E. coli* strain by 7% after 24 h of treatment which showed that almost all bacteria were alive after 24 h. On the other hand, the CS-CuO hybrid inactivated the *E. coli* strain by 99% after 6 h of treatment. Under the same conditions only 0.7% of survivors were found after 12 h, and complete reduction was observed at 24 h. To visualize the result, the digital photographs of control and *E. coli* treated with CS-CuO hybrids for 12 h (since the bacteria grow in

Table 1: Antibacterial activity of CS-CuO hybrid against *E. coli*.

Incubation time (h)	CS		CS-CuO	
	CFU (mL^{-1})	Reduction in viability (%)	CFU (mL^{-1})	Reduction in viability (%)
0	28×10^5	0	28×10^5	0
6	6.9×10^5	75.36	27×10^3	99.0
12	1.1×10^6	60.72	19×10^3	99.3
18	1.9×10^6	32.15	11×10^3	99.6
24	2.6×10^6	7.15	2×10^2	99.9

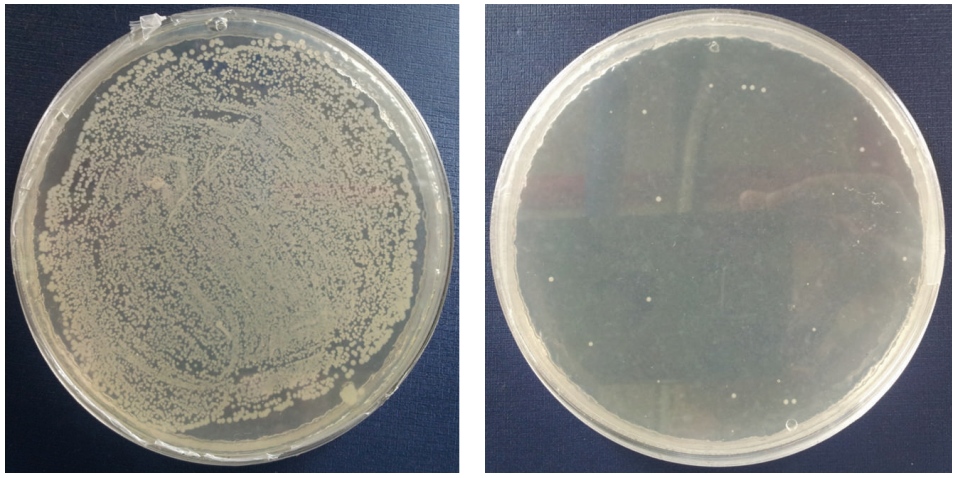

(a) (b)

Figure 7: Digital photographs of *E. coli* (a) without and (b) with CS-CuO hybrid for 12 h.

12 h) are shown in the Figure 7. The result indicated that the excellent reduction in the growth of bacteria confirmed the enhanced antibacterial activity of the hybrid. The *E. coli* tended to be inactivated in a similar manner regarding the time of treatment. The antimicrobial mechanism of the CS was attributed to the interaction with the strongly electronegative microbial surface [16]. The CS doped with CuO showed enhanced antibacterial activity which perhaps attributed to the synergistic effect of the CS and CuO nanoparticles. The Gram-negative bacteria have a thin layer of peptidoglycan and more complex cell wall with two cell membranes and outer membrane and a plasma membrane. The positively charged CS-CuO hybrid interacts with negatively charged lipidic bacterial membrane and thus changes its permeability, blocking the cells from nutrient intake, and thus ultimately affecting the cell growth and viability. It is also worth noting that the potential antibacterial activity of CS-CuO hybrid could be due to reactive oxygen species generation by the nanoparticles attached to the bacterial cells, which in turn provoked an enhancement of intracellular oxidative stress [10]. Therefore, our system showed much more efficient bactericidal activity for the sterilization of *E. coli* in an ordinary living space.

4. Conclusion

In this study, the CS-CuO hybrid was prepared by chemical precipitation method. The FT-IR spectrum endorsed the formation of hybrid. The thermal stability and crystallinity of the hybrid were studied by XRD and TGA. Zeta potential and TEM analysis confirmed the immobilization of CuO nanoparticle on the surface of CS. The hybrid catalyst showed a high photocatalytic activity of 84% for the photodegradation of the MB dye under UV-light irradiation for 30 min. The result showed that the repeated use of recycled CS-CuO hybrid (three times) did not affect its photocatalytic activity significantly. In addition, the hybrid material exhibited a superior antibacterial activity of 99% within 6 h of treatment against *E. coli* which was measured by CFU.

Acknowledgment

This research was supported by Basic Science Research Program through the National Research Foundation of Korea (NRF) funded by the Ministry of Education, Science and Technology (2012009529).

References

[1] C. Burda, X. B. Chen, R. Narayanan, and M. A. El-Sayed, "Chemistry and properties of nanocrystals of different shapes," *Chemical Reviews*, vol. 105, no. 4, pp. 1025–1102, 2005.

[2] S. J. Guo and E. K. Wang, "Functional micro/nanostructures: simple synthesis and application in sensors, fuel cells, and gene delivery," *Accounts of Chemical Research*, vol. 44, no. 7, pp. 491–500, 2011.

[3] X. Zhao, L. Lv, B. Pan, W. Zhang, S. Zhang, and Q. Zhang, "Polymer-supported nanocomposites for environmental application: a review," *Chemical Engineering Journal*, vol. 170, no. 2-3, pp. 381–394, 2011.

[4] S. Sarkar, E. Guibal, F. Quignard, and A. K. SenGupta, "Polymer-supported metals and metal oxide nanoparticles: synthesis, characterization, and applications," *Journal of Nanoparticle Research*, vol. 14, no. 2, article 715, 2012.

[5] J. D. Torres, E. A. Faria, J. R. SouzaDe, and A. G. S. Prado, "Preparation of photoactive chitosan-niobium (V) oxide composites for dye degradation," *Journal of Photochemistry and Photobiology A*, vol. 182, no. 2, pp. 202–206, 2006.

[6] E. I. Rabea, M. E.-T. Badawy, C. V. Stevens, G. Smagghe, and W. Steurbaut, "Chitosan as antimicrobial agent: applications and mode of action," *Biomacromolecules*, vol. 4, no. 6, pp. 1457–1465, 2003.

[7] Z. Liu, H. Bai, and D. D. Sun, "Facile fabrication of porous chitosan/TiO_2/Fe_3O_3 microspheres with multifunction for water purifications," *New Journal of Chemistry*, vol. 35, no. 1, pp. 137–140, 2011.

[8] V. Singh, A. K. Sharma, and R. Sanghi, "Poly(acrylamide) functionalized chitosan: an efficient adsorbent for azo dyes from aqueous solutions," *Journal of Hazardous Materials*, vol. 166, no. 1, pp. 327–335, 2009.

[9] V. Singh, A. K. Sharma, D. N. Tripathi, and R. Sanghi, "Poly(methylmethacrylate) grafted chitosan: an efficient adsorbent for anionic azo dyes," *Journal of Hazardous Materials*, vol. 161, no. 2-3, pp. 955–966, 2009.

[10] G. Applerot, J. Lellouche, A. Lipovsky et al., "Understanding the antibacterial mechanism of CuO nanoparticles: revealing the route of induced oxidative stress," *Small*, vol. 8, no. 21, pp. 3326–3337, 2012.

[11] G. Ren, D. Hu, E. W. C. Cheng, M. A. Vargas-Reus, P. Reip, and R. P. Allaker, "Characterisation of copper oxide nanoparticles for antimicrobial applications," *International Journal of Antimicrobial Agents*, vol. 33, no. 6, pp. 587–590, 2009.

[12] X. C. Jiang, T. Herricks, and Y. N. Xia, "CuO nanowires can be synthesized by heating copper substrates in air," *Nano Letters*, vol. 2, no. 12, pp. 1333–1338, 2002.

[13] M. H. Cao, C. W. Hu, Y. H. Wang et al., "A controllable synthetic route to Cu, Cu_2O, and CuO nanotubes and nanorods," *Chemical Communications*, vol. 9, no. 15, pp. 1884–1885, 2003.

[14] Z. L. Wang, X. Y. Kong, X. Wen, and S. Yang, "In situ structure evolution from $Cu(OH)_2$ nanobelts to copper nanowires," *Journal of Physical Chemistry B*, vol. 107, no. 33, pp. 8275–8280, 2003.

[15] C. K. Xu, Y. K. Liu, G. D. Xu, and G. H. Wang, "Preparation and characterization of CuO nanorods by thermal decomposition of CuC_2O_4 precursor," *Materials Research Bulletin*, vol. 37, no. 14, pp. 2365–2372, 2002.

[16] M. Gouda and A. Hebeish, "Preparation and evaluation of CuO/chitosan nanocomposite for antibacterial finishing cotton fabric," *Journal of Industrial Textiles*, vol. 39, no. 3, pp. 203–214, 2010.

[17] Y. Haldorai and J.-J. Shim, "Chitosan-zinc oxide hybrid composite for enhanced dye degradation and antibacterial activity," *Composite Interfaces*, vol. 20, no. 5, pp. 365–377, 2013.

[18] A. Higazy, M. Hashem, A. ElShafei, N. Shaker, and M. A. Hady, "Development of antimicrobial jute packaging using chitosan and chitosan-metal complex," *Carbohydrate Polymers*, vol. 79, no. 4, pp. 867–874, 2010.

[19] L.-H. Li, J.-C. Deng, H.-R. Deng, Z.-L. Liu, and X.-L. Li, "Preparation, characterization and antimicrobial activities of chitosan/Ag/ZnO blend films," *Chemical Engineering Journal*, vol. 160, no. 1, pp. 378–382, 2010.

[20] S. Sepulveda-Guzman, B. Reeja-Jayan, E. de la Rosa, A. Torres-Castro, V. Gonzalez-Gonzalez, and M. Jose-Yacaman, "Synthesis of assembled ZnO structures by precipitation method in aqueous media," *Materials Chemistry and Physics*, vol. 115, no. 1, pp. 172–178, 2009.

[21] F. Tian, Y. Liu, K. Hu, and B. Zhao, "The depolymerization mechanism of chitosan by hydrogen peroxide," *Journal of Materials Science*, vol. 38, no. 23, pp. 4709–4712, 2003.

[22] A. Rahnama and M. Gharagozlou, "Preparation and properties of semiconductor CuO nanoparticles via a simple precipitation method at different reaction temperatures," *Optical and Quantum Electronics*, vol. 44, no. 6-7, pp. 313–322, 2012.

[23] L.-H. Li, J.-C. Deng, H.-R. Deng, Z.-L. Liu, and L. Xin, "Synthesis and characterization of chitosan/ZnO nanoparticle composite membranes," *Carbohydrate Research*, vol. 345, no. 8, pp. 994–998, 2010.

[24] Y. Li, Y. Wei, G. Shi, Y. Xian, and L. Jin, "Facile synthesis of leaf-like CuO nanoparticles and their application on glucose biosensor," *Electroanalysis*, vol. 23, no. 2, pp. 497–502, 2011.

[25] C. Peniche-Covas, W. Argüelles-Monal, and J. San Román, "A kinetic study of the thermal degradation of chitosan and a mercaptan derivative of chitosan," *Polymer Degradation and Stability*, vol. 39, no. 1, pp. 21–28, 1993.

[26] H. Yu, J. Yu, S. Liu, and S. Mann, "Template-free hydrothermal synthesis of CuO/Cu_2O composite hollow microspheres," *Chemistry of Materials*, vol. 19, no. 17, pp. 4327–4334, 2007.

[27] A. Aguiar and A. Ferraz, "Fe^{3+}- and Cu^{2+}-reduction by phenol derivatives associated with Azure B degradation in Fenton-like reactions," *Chemosphere*, vol. 66, no. 5, pp. 947–954, 2007.